ANALYSIS AND OPTIMIZATION OF FELS WITH IRREGULAR WAVEGUIDES

Vitaliy Goryashko *, IRE NASU, Kharkov, Ukraine

Abstract

Using a time-dependent approach the analysis and optimization of a planar FEL-amplifier with an axial magnetic field and an irregular waveguide is performed. By applying methods of nonlinear dynamics three-dimensional equations of motion and the excitation equation are partly integrated in an analytical way. As a result, a self-consistent reduced model of the FEL is built in special phase space. The reduced model is the generalization of the Colson-Bonifacio model and takes into account the intricate dynamics of electrons in the pump magnetic field and the intramode scattering in the irregular waveguide. The reduced model and concepts of evolutionary computation are used to find optimal waveguide profiles. The numerical simulation of the original non-simplified model is performed to check the effectiveness of found optimal profiles. The FEL parameters are chosen to be close to the parameters of the experiment (*S. Cheng et al. IEEE Trans. Plasma Sci. 1996, vol. 24, p. 750*), in which a sheet electron beam with the moderate thickness interacts with the TE_{01} mode of a rectangular waveguide. The results strongly indicate that one can improve the efficiency by a factor of five or six if the FEL operates in the magnetoresonance regime and if the irregular waveguide with the optimized profile is used.

INTRODUCTION

The recent progress in the theory and experiment of free-electron lasers (FELs) and gyrotrons [1, 2] with Bragg cavities is strongly indicative that the application of novel electrodynamical structures provides the opportunity to realize unique properties of FELs to a large measure. For example, Bragg cavities, which are periodic arrays of varying dielectric or metallic structures, stimulate interest in traditional microwave applications because they can be built oversized (quasioptical) and, therefore, employed at higher frequencies and higher power. At the same time the investigation of traveling wave tubes (TWT) [3] shows that the TWT efficiency based on a regular (along the interaction region) electrodynamical structure is far from its possible maximal value. In fact, the difference between the cold phase velocity and the average velocity of the beam is the control parameter of the beam-wave interaction. By changing this parameter along the interaction region one can control the beam bunching and the energy transfer between bunches and microwaves. The local variation of the cold phase velocity along the region depends on the local variation in the waveguide profile. Then, in an effort to control the beam-wave interaction and improve the efficiency one should use irregular electrodynamic structures. Specifically, the combination of Bragg reflectors [4] and the section of an irregular waveguide seems to be a promising electrodynamic structure for a high-efficiency powerful FEL. The analysis of a planar FEL-amplifier with an axial magnetic field and an irregular waveguide is the topic of the present paper. This FEL configuration attracts out interest because it is well known that through the use of the axial magnetic field one can substantially improve the efficiency, as the cyclotron frequency tends to the undulator frequency [5, 6].

* vitgor06@mail.ru; vitgor@ire.kharkov.ua

THE MODEL

Let a sheet relativistic electron beam be injected into an irregular waveguide located in the external pump magnetic field that consists of the magnetic field of a linearly polarized (planar) undulator and a uniform axial magnetic field (see Fig. 1). The pump magnetic field is given by the vector-potential:

$$A_x^p(\vec{r}) = (B_u/k_u)\cosh(k_u y)\cos(k_u z) + B_\| y. \qquad (1)$$

Here $B_\|$ is the uniform axial guide field, B_u is the magnitude of the planar undulator field, $k_u = 2\pi/\lambda_u$ and λ_u are the wave number and the period of the undulator, respectively. In numerical simulations we model the injection of the electron beam into the interaction region by allowing the undulator amplitude to increase adiabatically from zero to a constant level over N_u undulator periods [7]. The unmodulated electron beam enters the interaction region, $z \in [0, L]$, with average longitudinal velocity $V_\|$. The irregular waveguide boundaries are set by expressions: $x = \pm a/2$ and $y = \pm w(z)/2$ ($a \gg w$), where $w(z)$ describes the varying distance between two wide walls of the waveguide, and $w'(0) = w'(L) = 0$. Let the FEL-amplifier be seeded by the TE_{01} mode, which is resonant (synchronous) with the electron beam, the mode frequency

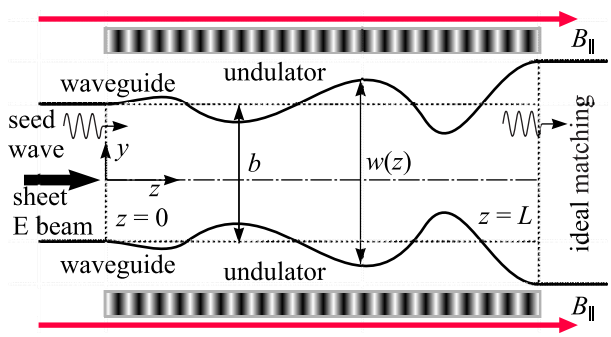

Figure 1: Sketch of the FEL in the $x = 0$ cross section.

and the amplitude at the input into the interaction region ($z = 0$) equaling ω and V_0, respectively. We consider that the interaction region is ideally matched to the regular output waveguide at the section $z = L$.

We will ignore scattering of the seed TE_{01} mode to higher modes and as well as the mode generation by the electron beam; then the evolution of the signal TE_{01} mode is governed by the x-component of vector-potential A_x^s:

$$A_x^s(\vec{r},t) = \mathrm{Re}\Big\{V(z,t)\sqrt{\frac{b}{w(z)}}\cos\Big(\frac{\pi y}{w(z)}\Big)\,e^{-i\omega t}\Big\}. \quad (2)$$

Here $V(z,t)$ is the slow-in-time amplitude satisfying the equation

$$\Big\{\frac{\partial^2}{\partial z^2}+k_z^2+\frac{2ik_z}{v_{gr}}\frac{\partial}{\partial t}\Big\}V(z,t) = -\frac{8\omega}{Sc}\frac{\sqrt{b}}{\sqrt{w(z)}}\int\limits_{-a/2}^{a/2}dx\times$$
$$\int\limits_{-w(z)/2}^{w(z)/2}dy\int\limits_{t-\pi/\omega}^{t+\pi/\omega}dt'\,j_x(\vec{r},t')\cos\Big(\frac{\pi y}{w(z)}\Big)e^{i\omega t'}, \quad (3)$$

where

$$k_z^2(z) = \frac{\omega^2}{c^2} - \Big(\frac{\pi}{w(z)}\Big)^2 - \Big(\frac{w'(z)}{2w(z)}\Big)^2\Big[1+\frac{\pi^2}{3}\Big]$$

is the wave number squared, $v_{gr}(z,\omega) = (dk_z/d\omega)^{-1}$ is the group velocity, c is the speed of light and $S = a \times b$. The boundary conditions read

$$\Big(\frac{\partial V}{\partial z} + ik_zV - \frac{1}{v_{gr}}\frac{\partial V}{\partial t}\Big)\Big|_{z=0} = 2ik_zV_0,$$
$$\Big(\frac{\partial V}{\partial z} - ik_zV + \frac{1}{v_{gr}}\frac{\partial V}{\partial t}\Big)\Big|_{z=L} = 0. \quad (4)$$

The microscopic current density is given by the following sum over electron trajectories, [7]:

$$\vec{j}(\vec{r},t) = \frac{I_0}{S_b}\int\limits_{-X_b/2}^{X_b/2}dx_0\int\limits_{-Y_b/2}^{Y_b/2}dy_0\int\limits_{t-L/V_\parallel}^{t}dt_e\frac{\vec{p}(z;\vec{r}_{\perp 0},t_e)}{p_z(z;\vec{r}_{\perp 0},t_e)}\times$$
$$\delta[\vec{r}_\perp - \vec{r}_\perp(z;\vec{r}_{\perp 0},t_e)]\delta[t - t(z;\vec{r}_{\perp 0},t_e)], \quad (5)$$

where I_0 is the beam current at the input into the interaction region; $S_b = X_bY_b$ is the cross sectional area of the beam; $\vec{p}(z;\vec{r}_{\perp 0},t_e)$ and $\vec{r}_\perp(z;\vec{r}_{\perp 0},t_e)$ are the mechanical momentum and the transverse coordinate, respectively; $t(z;\vec{r}_{\perp 0},t_e)$ is the arrival time of an electron at the position z; t_e and $\vec{r}_{\perp 0} = \vec{r}_{\perp 0}(x_0,y_0)$ are the entrance time and the transverse coordinates, which the electron has at the input of the interaction region. The sheet electron beam is lying from $x_0 = -X_b/2$ to $x_0 = X_b/2$ and from $y_0 = -Y_b/2$ to $y_0 = Y_b/2$ in the x and y directions, respectively. Since the relativistic beam-wave interaction is being studied, the nonradiated fields (space-charge fields) are supposed to be negligible. The relativistic effects result in that force f_m caused by the nonradiated magnetic field partially suppresses the defocusing action of the transversal part of force $f_e^{(pot)}$ caused by the potential part of the nonradiated electric field, the axial component of $f_e^{(pot)}$ being partially compensated by force $f_e^{(rot)}$ caused by the rotational part of the nonradiated electric field (see [8] for details).

The motion of a typical electron within the electron beam can be described by the relativistic Hamiltonian

$$\mathcal{H} = \sqrt{m_e^2c^4 + \big(c\vec{P} - e\vec{A}^p - e\vec{A}^s\big)^2} = m_e\gamma c^2. \quad (6)$$

Here e and m_e are the electron charge and rest mass, respectively; the canonical momentum $\vec{P}$ is related to the mechanical momentum $\vec{p}$ by $\vec{P} = \vec{p} + (e/c)(\vec{A}^p + \vec{A}^s)$. The initial conditions for the mechanical momentum and coordinates read:

$$p_x|_{t=t_e} = p_y|_{t=t_e} = 0, \quad p_z|_{t=t_e} = \mathcal{E}V_\parallel/c^2,$$
$$x|_{t=t_e} = x_0, \quad y|_{t=t_e} = y_0, \quad z|_{t=t_e} = 0, \quad (7)$$

where $\mathcal{E}$ is the initial energy of the electron entering the interaction region at the time t_e. The excitation equation (3) along with the expression for the current density (5) and the equations of motion generated by the Hamiltonian (6) describe the electron-wave interaction in the studied FEL in a self-consistent way.

CONTROL OF THE BEAM-WAVE INTERACTION

In order to find the parameters and the waveguide profile that provide the maximal efficiency one has to apply an optimization technique. However, the direct numerical optimization based on the non-averaged FEL model fails to work because a vast amount of computational resources is required. Typically, about several thousand equations of motions and the partial differential equation for the wave amplitude have to be simulated. In this paper I propose another approach to the problem. The investigation is divided into several stages: initially equations of motion and the excitation equation are partly integrated in an analytical way using methods of nonlinear dynamics. As a result, the universal reduced FEL model is derived in special phase space. Then with this model and some principles of evolutionary computations (genetic algorithms) the numerical optimization of the waveguide profile is performed. Finally, the simulation of the non-simplified original model using the found optimal waveguide profiles is carried out. So, one can come closer to understanding of what increase in the efficiency can be achieved in practise. For lack of the paper space let us go straight to the numerical results of the optimization for a practical example (for details see [9]).

The FEL parameters are chosen to be close to the parameters of the experiment [10]: 450-kV beam voltage, $|I_0| = 16$-A beam current, 1.0 mm $\times$ 2.0 cm sheet beam interacts with the TE_{01} mode (the field varying along the narrow wall) of the 4.5 mm $\times$ 6.0 cm rectangular waveguide.

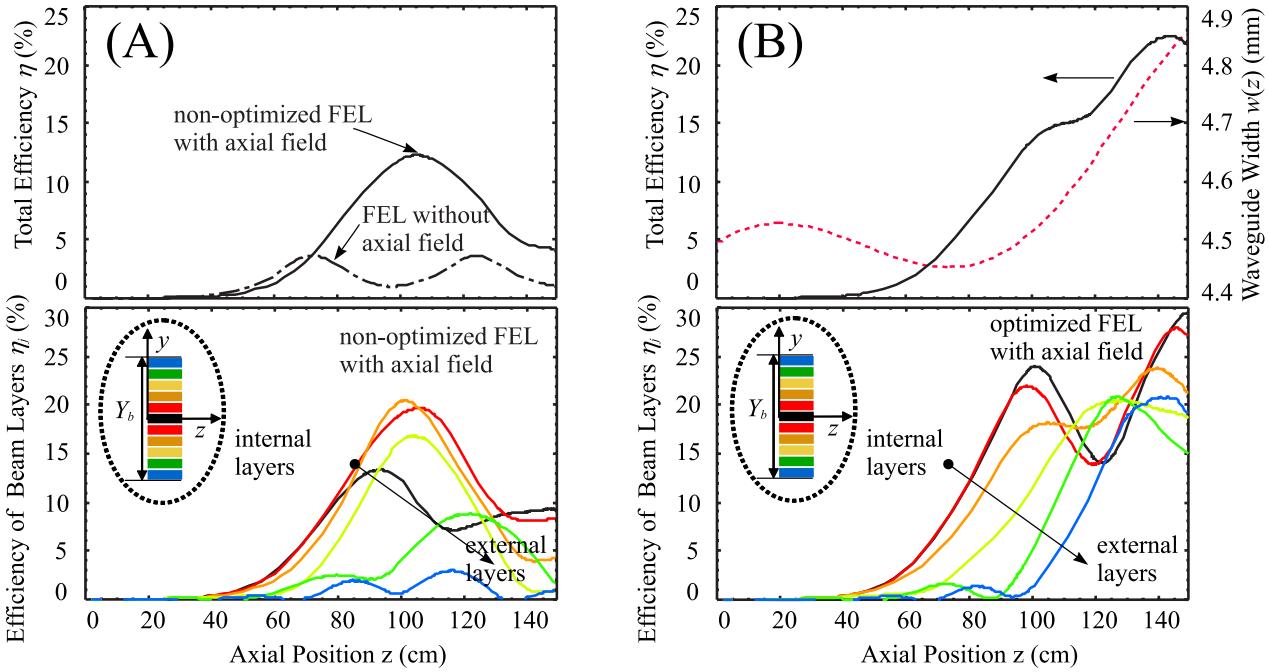

Figure 2: The FEL efficiency and waveguide width vs. the interaction length. The results of the non-simplified model simulation are demonstrated.

The undulator magnitude increases adiabatically within six periods and the undulator is characterized by $B_u = 3.5$ kG and $\lambda_u = 1.0$ cm in the regular region. A 1.5-kW input signal with the 4.2 mm wavelength is injected. In our simulation we assume that there is the axial magnetic field 20 kG as well. The wavelength is slightly different from that in the experiment because of the different average axial velocity. The results of our simulation code were verified against of those of the paper [10] and an excellent agreement was found. Indeed, according to the experiment [10], the non-optimized FEL without the axial magnetic field approaches saturation at a wiggler length of 71 cm with a gain of 24 dB at a 1 kW input power, whereas, according to our simulations (see also Fig. 2A), the FEL approaches saturation at a length of 74 cm with a gain of 25 dB.

From Fig. 2A we see that using the magnetoresonance effect we can significantly enhance the efficiency. It was 4% efficiency without the axial field in the experiment and it is 12% efficiency with the axial magnetic field. However, there is a weak interaction between the external beam layers and the microwave because different layers of the electron beam have different 'transverse' detuning with the wave due to the transverse inhomogeneity of the pump magnetic field. Geometric positions of different beam layers at the beginning of the interaction region are shown inside the dotted ellipse. The black curve is for the central layer. Other layers are displaced with respect to the symmetry plane $y = 0$.

In Fig. 2B the results for the optimized FEL with the axial field are presented. The maximal relative deviation of the waveguide width is 8% and the maximal and minimal widths are around 4.9 mm and 4.4 mm, respectively. The dimensionless slope of the taper $\epsilon_w = k_u^{-1}\partial_z \ln w \approx 0.0002$ is much smaller than the normalized growth rate of the wave $\mathrm{Im}\delta k_z/k_u \approx 0.0029$. Therefore, our model, based on the approximation in which mode-mode coupling terms are neglected in the large signal equations, seems to be reasonable. Using the waveguide with the optimized profile one can double the efficiency so that the final efficiency is around 22%. We also see that the external layers interact with the wave much more effectively in the optimized FEL. So, by changing the waveguide profile we regulate the phase shift between a ponderomotive current and a ponderomotive wave thus controlling the beam-wave interaction and increasing the FEL efficiency. It is checked that the proposed FEL-amplifier reaches steady-state regime and it takes around 200 ns.

It should be mentioned that the applied axial magnetic field $\vec{B}_\parallel$ not only allows one to increase the FEL efficiency substantially, but also causes a beam divergence due to the electron drift $\vec{B}_\parallel \times \nabla \vec{B}_u$ ($\vec{B}_u$ is the undulator field) in the x-direction. However, ponderomotive potential W is independent of x-coordinates of electrons because the microwave and pump magnetic field are homogeneous in the x-direction. As a result, the beam-wave interaction is not drift-dependent unless electrons fall down on the waveguide walls. It is checked that electrons do no touch the walls in the situations of interest (see Fig. 3). Since the drift velocity depends on y_0 as $\sinh[k_u y_0]$ the central layer $y_0 = 0$ does not undergo the drift effect, whereas the beam layers displaced with respect to the symmetry plane $y = 0$ drift toward walls with different velocities.

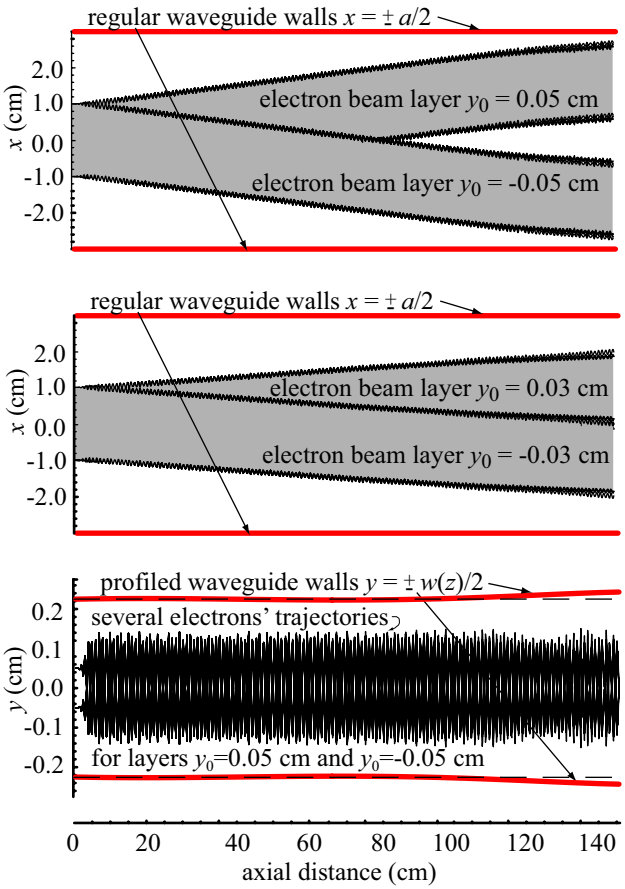

Figure 3: Some electrons' trajectories in the x-z and y-z planes are shown.

Depending on specific parameters, a number of parasitic modes, including a mixture of the TE_{21} and TM_{21} modes, may be excited by the beam. However, for the given above FEL configuration parasitic modes affect weakly interaction of the beam with the dominant TE_{01} mode due to several reasons. Coupling between the wave and the beam strongly depends on the electric field distribution in the transverse plane and the beam location. From Fig. 4 we see that the beam position coincides with the field maximum for the TE_{01} mode and the field distribution is homogeneous in the x-direction, therefore the beam-wave coupling is high. But the contributions of different parts of the beam annihilate each other for TE_{11} and TM_{11} because the electric field E_x (E_y) has different signs for $x > 0$ ($y > 0$) and $x < 0$ ($y < 0$). As for the TE_{21} and TM_{21} modes, these modes are quite effectively matched to the beam via E_x, but their resonant frequency is 68.5 GHz whereas the FEL is seed at the frequency 71.4 GHz and the bunching occurs at a higher frequency than it is necessary for the excitation of TE_{21} and TM_{21} modes. In the experiment [11] the output power from the tapered wiggler was nearly all (∼90%) in the fundamental mode whereas the resonant frequencies for the TE_{01} and TE_{21} modes were 34.6 and 32.5 GHz, respectively. Moreover, it was not reported about the parasitic modes excitation in experiment [10]. Besides, the beam drift leads to suppression of the TE_{21}-TM_{21} modes excitation because, as we see from Fig. 3 and Fig. 4, at the end of the interaction region the phase shift between the external beam layers $y_0 = \pm 0.05$ mm and the central layer $y_0 = 0$ is around π. Therefore, the contribution of the different layers is partly annihilated and we may ignore parasitic modes.

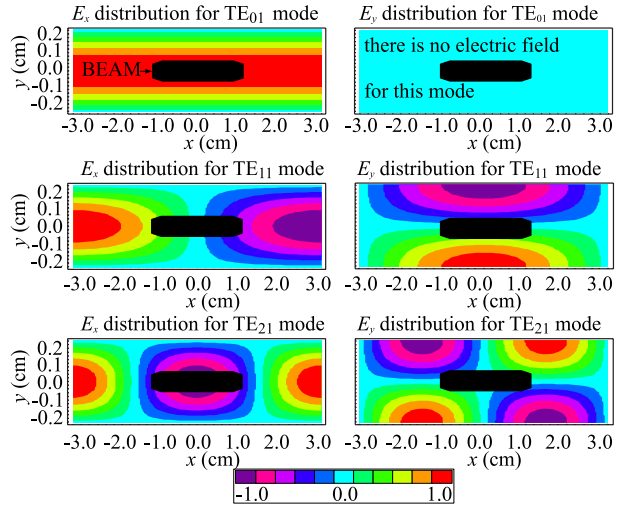

Figure 4: The field distributions of TE_{01}, TE_{11}, TE_{11} modes and the beam initial position are demonstrated.

CONCLUSION

The operation of the planar FEL-amplifier with the axial magnetic field and the irregular waveguide is studied in a self-consistent way. It is shown that one can increase the efficiency by a factor of five or six if the FEL operates in the magnetoresonance regime and if the irregular waveguide with the optimized profile is used

REFERENCES

[1] N.S. Ginzburg et al., Phys. Rev. Lett. 84 (2000) 3574.

[2] J.R. Sirigiri et al., Phys. Rev. Lett. 86 (2001) 5628.

[3] V.F. Kravchenko, A.A. Kuraev, A.K. Sinitsyn, Physics-Uspekhi 50 (2007) 489.

[4] V.L. Bratman, G.G. Denisov, N.S. Ginzburg, M.I. Petelin, IEEE J. Quantum Electron., QE-19 (1983) 282.

[5] P. Sprangle, V.L. Granatstein, Phys. Rev. A 17 (1978) 1792.

[6] V.A. Goryashko, K. Ilyenko, A. Opanasenko, Phys. Rev. ST Accel. Beams 12 (2009) 100701.

[7] H.P. Freund, H. Bluem. C.L. Chang, Phys. Rev. A 36 (1987) 2182.

[8] V.A. Goryashko, K. Ilyenko, A.N. Opanasenko, Nucl. Instr. and Meth. A 620 (2010) 462.

[9] V.A. Goryashko, http://arxiv.org/abs/1004.1373.

[10] J.H. Booske et al., Phys. Plasmas 1 (1996) 1714.

[11] T.J. Orzechowski et al., Phys. Rev. Lett. 57 (1986) 2172.